Investigating future changes of Antarctic Intermediate Water formation in CESM1

STEPHANIE PENNINGTON
Department of Atmospheric and Oceanic Science, University of Maryland, College Park

CORINNE HARTIN
Joint Global Change Research Institute, College Park

|

May 16, 2017

ABSTRACT

Antarctic Intermediate Water (AAIW), formed primarily in the Southern Ocean, is an important water mass responsible for nutrient transport, heat storage, and uptake of anthropogenic CO_2 throughout the global oceans. AAIW is also thought to be the most important global source of O_2 and nutrient transfer to the equatorial regions (Russell and Dickson 2003). In this study we investigate changes in the surface properties of AAIW in the South Pacific, under historical (1970-1990) and RCP8.5 (2080-2100) scenarios, using the Community Earth System Model (CESM-BGC). These surface properties will then be subducted within intermediate water and distributed throughout the subtropical gyre. AAIW within the South Pacific is identified based on a low salinity of 34.2 psu. This study will investigate changes in AAIW surface properties (e.g., salinity, O_2, NO_3) and formation changes under the RCP 8.5 (+8.5 W/m^2 from pre-industrial values) scenario. Identifying changes in AAIW is valuable in understanding how the uptake of heat, freshwater, and CO2 may change within a changing climate.

INTRODUCTION

a. Motivation

Within the last century, greenhouse gas concentrations, like Carbon Dioxide (CO_2), have been rising due to the enhanced greenhouse gas effect. According to the Mauna Loa Observatory in Hawaii, current CO_2 levels are at 409.01 ppm and steadily rising. The ocean acts as an important carbon sink, accounting for about 48% of CO_2 fossil-fuel emission uptake (Sabine et al. 2004), mitigating a large portion of anthropogenic CO_2. However, changes in the formation of AAIW

due to climate change could disrupt this uptake and cause further intensification of the greenhouse gas effect.

b. AAIW formation and global importance

The Southern Ocean is home to a water mass that plays a significant role in the global climate system. Antarctic Intermediate Water (AAIW) is particularly important for nutrient transport (e.g. O_2, silica), heat storage, uptake of anthropogenic CO_2, and ventilation throughout the global ocean circulation. The formation of AAIW is the key process in the uptaking of these nutrients and CO_2. AAIW forms from upwelled Circumpolar Deep Water off the coast of Antarctica. This cold, low-salinity water, which is now at the surface, is referred to as Antarctic Surface Water (AASW). AASW then moves northward due to Ekman transport until it hits the Polar Front. At the Polar Front, the cold, low-salinity water meets warmer waters and subducts as AAIW at the Subantarctic Front (Sloyan and Rintoul 2001b). During this subduction, CO_2 and various nutrients enter AAIW through air-sea flux. Due to this, AAIW is thought to be one of the largest global transports of anthropogenic CO_2 (Ito et al. 2010).

c. Influence of the Antarctic Circumpolar Current

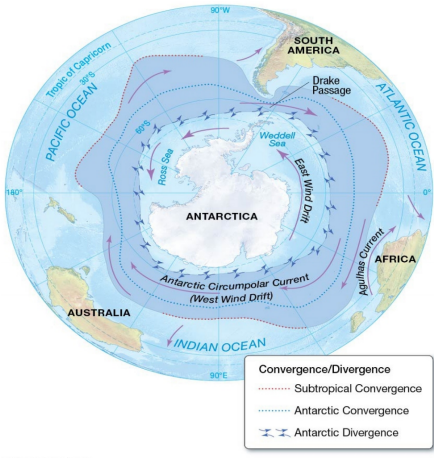

Figure 1. Polar view of Antarctica. Prevailing winds drive convergence and divergence at the surface, creating the Polar (Antarctic Convergence) and Subantarctic Front (Subtropical Convergence). (Pearson Education, Inc. 2011)

The transport of CO_2 and oxygen is facilitated by the Antarctic Circumpolar Current (ACC), a major current found in the Southern Ocean, which feeds into the Southern Hemisphere Subtropical gyres. This allows AAIW to spread and extend as far as 20°N (Talley 1999). The ACC is an eastward flowing, driven by strong westerly winds, current circling Antarctica that varies between the latitudes of 40 and 65°S. The ACC is bounded in the south by the convergence of polar easterlies and the strong prevailing westerlies, or what is referred to as the Polar Front. The north boundary is the Subtropical Convergence, where cold polar water meets warmer equatorial region waters, see **Figure 1.** The ACC is also unbounded by any landmass, with the exception of the narrow restriction at the Drake Passage, allowing for large volume transports and connection with all major ocean basins. The connection to all Southern Hemisphere ocean

basins, large nutrient uptake, and CO_2 transport allow this water mass to play a significant role in climate. A change in the formation and uptake of AAIW could have impacts to the global carbon cycle and be an important tool for diagnosing further change in the climate system.

d. AAIW properties

Water masses are defined by numerous factors, including temperature, salinity, potential density, and nutrient content. AAIW is characterized by a salinity minimum, cold temperatures, and high oxygen concentrations. Preliminary results have identified AAIW to be 34.2 psu (practical salinity units) and a surface density range of 26.6-27.2 kg/m^3. In **Figure 2**, we can distinctly see the low salinity waters, represented by the yellow and green colors, subducting at around 60°S. These values will be used as baseline conditions to compare with mid-century and end-of-century projections. Changes in the physical properties of AAIW could affect the formation and nutrient uptake. This study aims to identify and diagnose future changes at important uptake locations, such as Antarctic Intermediate Water, to assess potential decreases in ocean CO_2 and oxygen uptake and their implications.

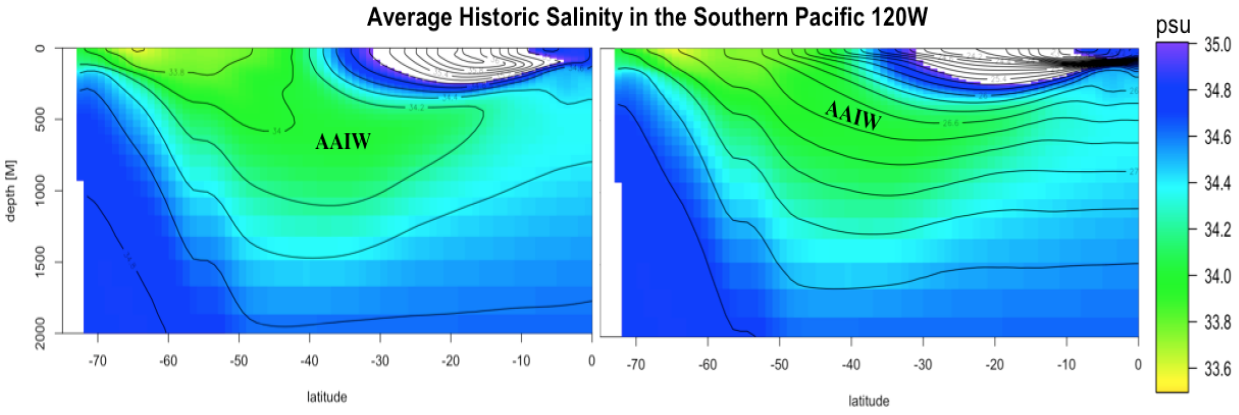

Figure 2. Both figures are showing historic salinity (psu) depth profiles at 120W from the surface to 2km, 80S to the equator. Areas of fresher water (lower salinity) are shown in yellow and green colors; areas of saltier water are shown in blue. a) (Left) Overlaid of lines of constant salinity indicate AAIW salinity to be 34.2psu. b) (Right) Overlaid lines of constant density indicate a surface density range of 26.6-27.2 kg/m^3.

METHODS

a. CESM1-BGC

This study uses the Community Earth System Model - Biogeochemical (CESM1-BGC) output. This is an open-source model developed for the Coupled Model Intercomparison Project, phase 5 (CMIP5) by the National Center for Atmospheric Research (NCAR) through the Department of Energy and the National Science Foundation.

CESM1 is the successor of the Community Climate System Model (CCSM4), which now offers a more interactive carbon cycle and improved sea ice component for Greenland and Antarctica climate prediction (Long et al. 2013). This is a fully coupled global climate model, which includes the land, atmosphere, ocean, and sea-ice featuring a 1° by 1° horizontal resolution and 60 vertical layers. The BGC component field was initialized using data based climatologies and is used to track biogeochemical cycles in the earth system, which will be valuable in tracking changes in AAIW uptake.

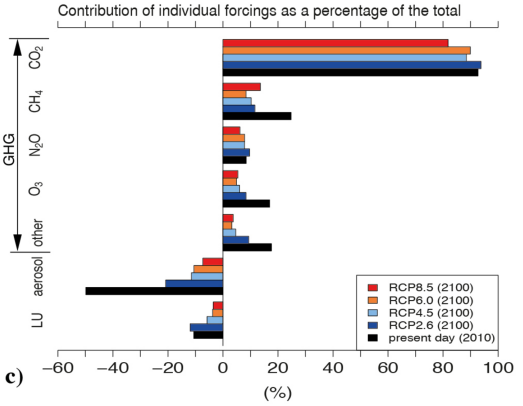

Greenhouse gases: CO2, methane, nitrous oxide, fluorocarbons, sulfur hexafluoride

Aerosols/chemically active gasses: Sulfur dioxide, soot, organic carbon, carbon monoxide, nitrogen oxides, volatile organic compounds, ammonia

Figure 3. a) Emission contributions of individual forcings as a percentage of the total for RCPs compared to present day contributions. b) List of greenhouse gases, aerosols, and chemically active gases included in RCP projections. (IPCC, 2013)

b. Representative Concentration Pathways (RCPs)

CESM1-BGC is forced by emission concentrations and run for various radiative forcing scenarios put forth by the Intergovernmental Panel on Climate Change (IPCC). These scenarios, called Representative Concentration Pathways (RCPs), were introduced in the IPCC's Fifth Assessment Report (AR5) and range from 2.6 W/m^2 to 8.5 W/m^2 radiative forcing by the end of the century (2100) (IPCC, 2014). Emission scenarios are trajectories of concentrations of greenhouse gases such as those shown in **Figure 3**. Figure 3 also shows a breakdown of each greenhouse gas and their percentage contribution

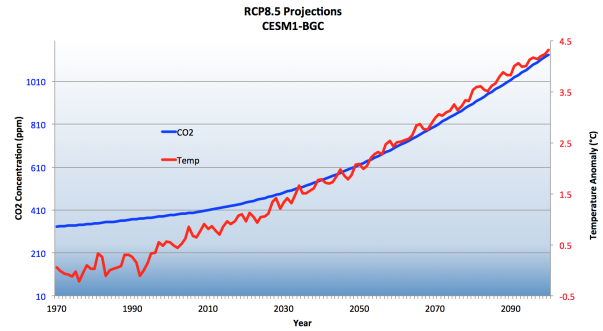

Figure 4. CESM1-BCG RCP8.5 projections for CO_2 and temperature anomaly from 1970 to 2100. Both indicate an increasing trend with 3XCO_2 of today's value and a 4°C increase by 2100.

to the total forcings. Carbon Dioxide is responsible for about 80% of the total forcings included in RCP 8.5. This study will focus on the RCP 8.5 scenario, which has been described as consistent with no policy change in emissions, essentially "business as usual". **Figure 4** shows the CESM1-BGC projections for the RCP 8.5 emission scenario from 1970 to 2100. We see a 4°C temperature anomaly and 3 x CO_2 by 2100. These changes are representative of the factors that influence changes in AAIW, which are evident in the results.

c. Data Processing

This study will look at changes in AAIW from historic values to mid-century and end-of-century projections using monthly ocean data from 1970-2100. The model output data was collected from Earth System Grid, a climate data distribution portal. We chose historic values to be from 1970-1990, mid-century from 2030-2050, and end-of-century from 2080-2100, see the summary provided in **Table 1**. Each 20-year time period was then averaged using Climate Data Operators (CDO). CDO offers the ability to format multiple aspects of a data files in one command.

Table 1. Model Used for Each Time Period

Label	Model	Ensemble	Year
Historic	CESM1-BGC	r1i1p1	1970-1990
Mid-Century	CESM1-BGC	r1i1p1	2030-2050
End-Of- Century	CESM1-BGC	r1i1p1	2080-2100

The 20-year periods were first selected, then averaged, and finally re-gridded to sort the longitudes to a 0-360° format. The resulting data files were plotted in RStudio using R language. We took depth profiles at four longitudes: 180W, 150W, 120W, and 90W, and surface plots of the South Pacific. This study will focus on 120W for simplicity since this longitude will give us average conditions of the South Pacific as it cuts through the middle of the subtropical gyre. Difference plots were also calculated for the physical surface properties of AAIW to show quantitative changes. These were calculated by subtracting historic values from end-of-century values.

d. Buoyancy Flux Calculation

Buoyancy plays an important role in the subduction of surface waters. Changes in fluxes of heat and freshwater from air-sea interactions modify surface densities. The buoyancy flux (B) from the atmosphere/ice to the ocean is calculated by:

$$B = (g/\rho_o)[\alpha Q_{net}/C_p - \beta S(P-E)] \quad \textbf{(1)}$$

where g is the acceleration due to gravity, ρ_o is the sea surface density, α is the thermal expansion coefficient, Q_{net} is the net heat flux into the ocean, C_p is the specific heat capacity of seawater, β is the haline contraction coefficient, S is the sea surface salinity, and P-E is the freshwater flux. A positive value for B indicates increased stratification while a negative value for B corresponds to subduction. Different plots were also calculated by subtracting historic values from end-of-century values.

e. Formation Rate Calculation

The thermodynamic approach involves looking at changes in the ocean properties of density, temperature, and salinity. The annual mean formation rate (M, in Sv) is calculated by:

$$M = -[F(\sigma_{\theta 2}) - F(\sigma_{\theta 1})] \quad \textbf{(2)}$$

Where F is the water mass transformation (subduction) rates, which are estimated using the formula shown in **Equation 3**. A positive value for M indicates subduction in the density range, and a negative value indicates subduction into a less dense range. The annual average formation rate (F) is calculated by integrating the annual subduction rate over the area of surface AAIW isopycnals that we found to be 26.6-27.2 kg/m^3:

$$F(\sigma_\theta) = -\frac{1}{\Delta\sigma}\iint_A \left(\frac{\alpha Q}{C_p}\right)dA + \frac{1}{\Delta\sigma}\iint_A \rho_s\left(\frac{\beta S(P-E)}{1-S}\right)dA \quad \textbf{(3)}$$

where $\Delta\sigma$ is the surface density difference.

RESULTS

a. Physical Property Changes

Figure 5a shows difference values plotted in the South Pacific Ocean. Projections show a density decrease of AAIW by about 0.3 kg/m^3. The density of seawater is dependent on salinity

and temperature properties, so we further diagnose this decrease by also looking at differences in salinity and temperature in the area. We see a salinity freshening of 0.2 psu and temperature increase of 2.5°C. The magnitude of the temperature change indicates that the density changes of surface AAIW are largely temperature dependent. Changes in surface density can hint at more complex interaction of changes in AAIW formation. Isopycnals of the surface properties of AAIW also show a poleward movement through the end of the century, see **Figure 5b**. These changes could indicate a possible expansion of the subtropical gyre (Zhang et al. 2014).

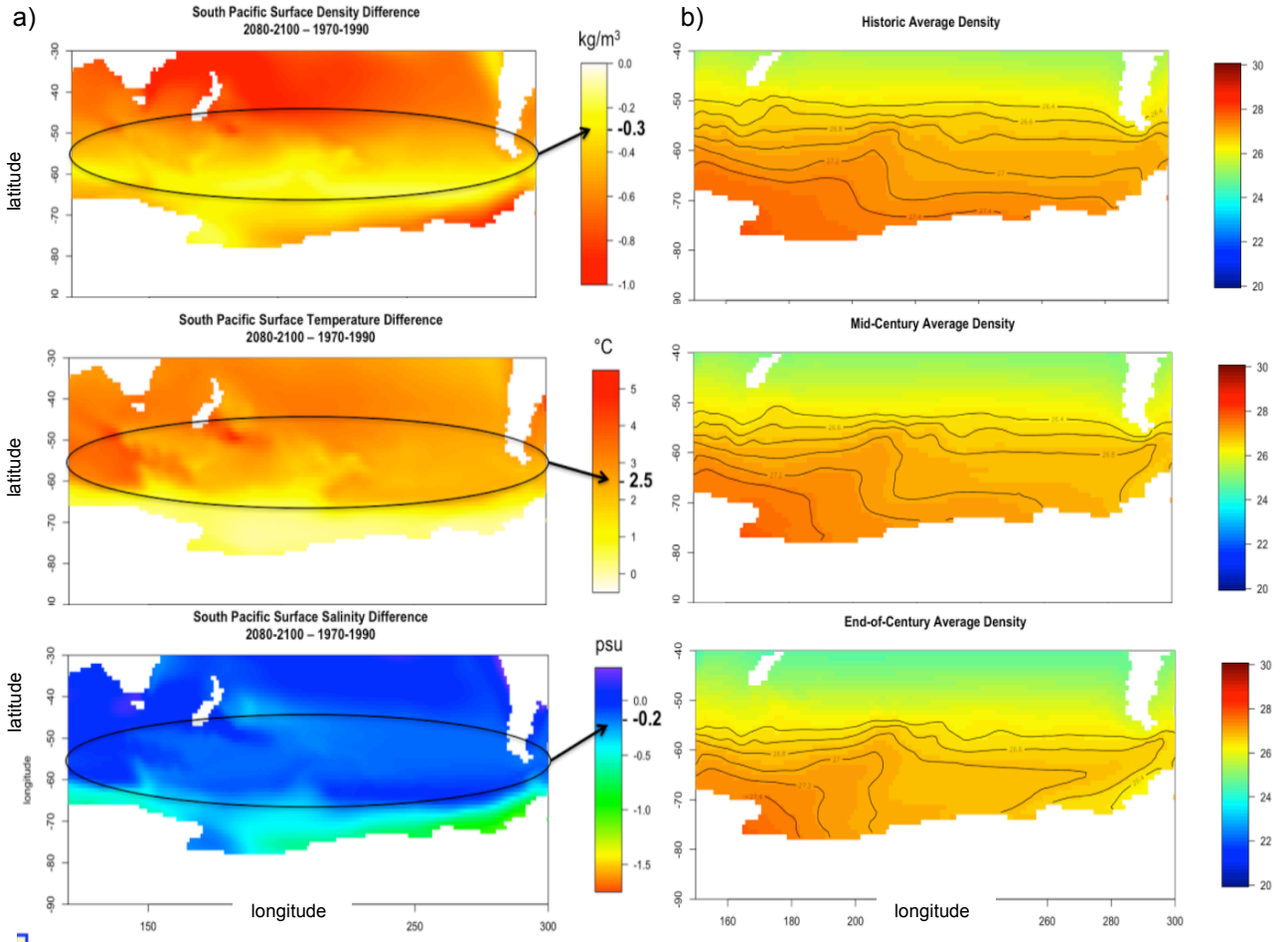

Figure 5. a) Difference plots of the South Pacific calculated for density, salinity, and temperature from 1970-2100. The black circle encompasses surface AAIW based on historic density values. b) Average surface density in the South Pacific through historic, mid-century, and end-of-century. Isopycnals overlaid to show boundary outcropping of surface AAIW.

Surface density changes can be further diagnosed by looking at freshwater flux and air-sea interactions. Freshwater flux, calculated as precipitation-evaporation, through the end-of-the-

century is shown to have increased from 55°S to the coast of Antarctica, see **Figure 6**. Sea-ice melt off the coast of Antarctica near the Ross Sea may also influence the freshwater flux, reducing ocean convection (Kirkman and Bitz, 2011). A positive flux of freshwater into a system would decrease sea surface salinity, making the water lighter and less willing to subduct. Air-sea fluxes can also be quantified by analyzing changes in wind stress. Wind stress is projected to increase in the Southern Hemisphere with a changing climate (Russell et al., 2006; Hartin 2012). Wind stress is found to have increased in the South Pacific by up to 0.06 N/m^2 below 50°S, see **Figure 7**. Since surface fluxes drive overturning, we can quantify these changes in the perspective of formation by calculating buoyancy flux, see **Equation 1**. A more buoyant surface would indicate areas where less water is subducting as AAIW. Areas of AAIW formation are found to have a positive buoyancy increase through the end-of-century suggesting a decrease in AAIW formation, see **Figure 8**.

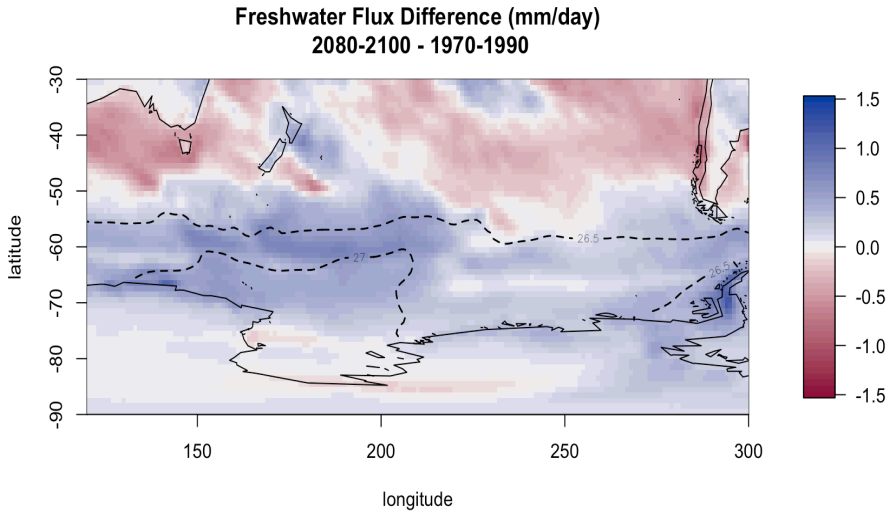

Figure 6 (right). Difference plot of average freshwater flux (precipitation-evaporation, mm/day) in the South Pacific from 1970-2100. Areas of blue correspond to positive flux or an increase in precipitation/decrease in evaporation and areas of red correspond to negative flux or an increase in evaporation/decrease in precipitation. End-of-century surface AAIW outcropping shown in black dashed lines.

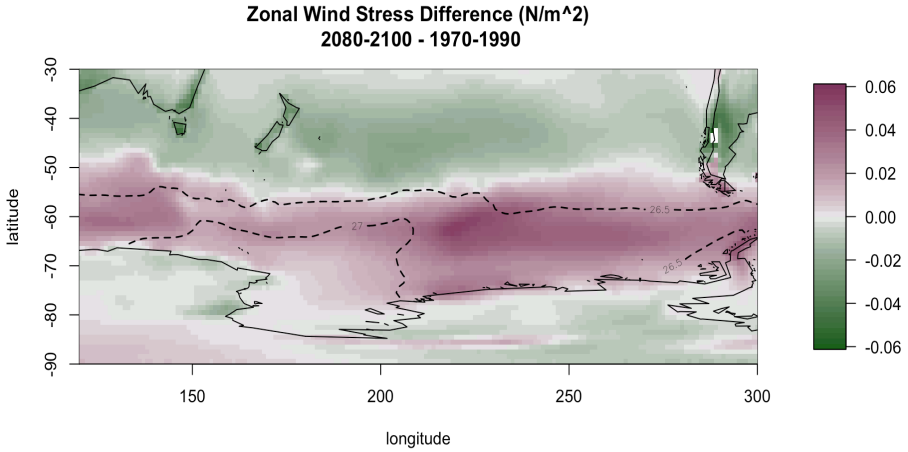

Figure 7 (left). Difference plot of average zonal wind stress, in N/m^2, in the South Pacific from 1970-2100. Areas of purple (positive) correspond to an increase in wind stress and areas of green (negative) correspond to decrease in wind stress through the end of the century. End-of-century surface AAIW outcropping shown in black dashed lines.

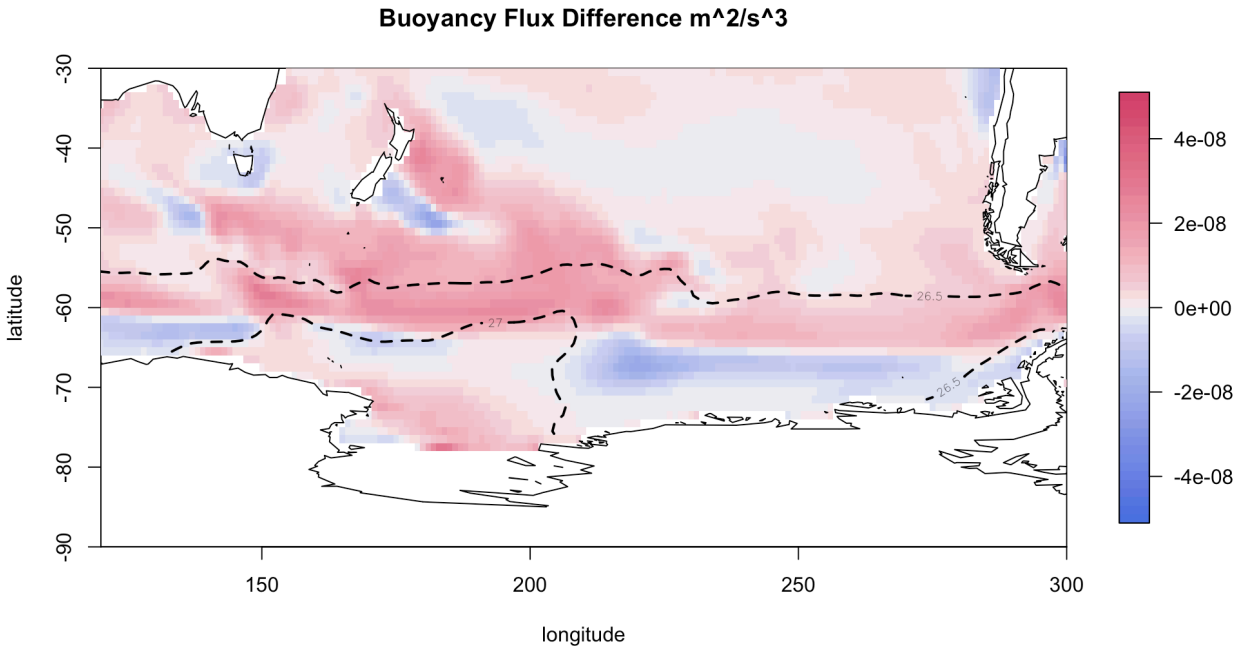

Figure 8. Difference plot of average buoyancy flux, in m^2/s^3, in the South Pacific from 1970-2100. Areas of red correspond to positive flux or an increase in stratification and areas of blue correspond to negative flux or subduction. End-of-century surface AAIW outcropping shown in black dashed lines.

Together, increased freshwater flux, zonal wind stress, and buoyancy flux in areas of AAIW formation suggest an increase in stratification of surface waters. Increased stratification would inhibit subduction and create low or negative formation rates. The thermodynamic method, see **Equation 3**, for calculating formation rates was chosen based on the increase seen in the surface water buoyancy fluxes. The formation rate calculates the total amount of freshwater and heat transfer between the AAIW density ranges of 26.6-27.2 kg/m^3. Formation rates for historic and RCP 8.5 end-of-century projections are summarized in **Table 2**. The results show a decrease in formation rate between the historical and end of century by 19.53 Sv. A decrease of this magnitude would have profound impacts on the formation of AAIW and general ocean circulation globally.

Table 2. Formation Rates, in Sverdrup

	Total (Sv)
Historic	21.11
RCP 8.5	1.58

CONCLUSION

The physical properties of AAIW (e.g. density, salinity, temperature) show significant changes towards less dense surface waters in the South Pacific. AAIW formation is projected to slow down by 19.53 Sv, with increases in buoyancy flux and freshwater flux. Formation rates are an important indicator of a change in the uptake of CO_2 and nutrients. A slowing of AAIW

formation could imply a disruption of uptake and promote further climate change. The ocean plays an important role in global climate, especially in the threat of anthropogenically produced warming.

FUTURE RESEARCH

Future research could involve the following projects:

A. **Analyzing other RCP scenarios under CESM1-BGC.** Studying of all possible scenarios to quantify AAIW formation in each radiative forcing scenario.
B. **Calculating formation rates of other important water masses in the South Pacific (e.g. SAMW).** Analysis of how accurate CESM1 models water masses in the South Pacific under a changing climate.
C. **Compare accuracy of formation rates in other CMIP5 models.** Evaluation of CESM1 in comparison to other CMIP5 models would expose limitations and uncertainties in CESM1.
D. **Compare methods of formation rates.** Analyzing the thermodynamic vs. dynamic method would address caveats to each method and potential discrepancies in the results.

ACKNOWLEDGEMENTS

This study is part of the University of Maryland Department of Atmospheric and Oceanic Science (AOSC) undergraduate thesis project. I would like to acknowledge the World Climate Research Programme's Working Group on Coupled Modeling, which is responsible for CMIP5, and also thank the National Science Foundation, Department of Energy, and National Center for Atmospheric Research (NCAR) for providing the CESM1-BGC model output through Earth System Grid. I would also like to recognize the American Meteorological Society (AMS) Committee on Polar Meteorology and Oceanography and AOSC department for funding to the AMS Annual Meeting in 2017. And finally, I would like to thank Dr. Tim Canty, of the AOSC department, and Dr. Corinne Hartin, of JGCRI, for their continued support and guidance.

REFERENCES

Downes, S. M., N. L. Bindoff, and S. R. Rintoul, 2009. Impacts of Climate Change on the Subduction of Mode and Intermediate Water Masses in the Southern Ocean. *J. Climate,* **22** , 3289-3302, doi: http://dx.doi.org/10.1175/2008JCLI2653.1.

Garabato, A. C. N., L. Jullion, D. P. Stevens, K. J. Heywood, and B. A. King, 2009. Variability of Subantarctic Mode Water and Antarctic Intermediate Water in the Drake Passage during the Late-Twentieth and Early-Twenty-First Centuries. *J. Climate*, **22** , 3661-3688,
doi: http://dx.doi.org/10.1175/2009JCLI2621.1.

Graham, J. A., D. P. Stevens, and K. J. Heywood, 2013. Nonlinear Climate Responses to Changes in Antarctic Intermediate Water. *J . Climate,* **26** , 9175–9193,
doi: http://dx.doi.org/10.1175/JCLI-D-12-00767.1.

Hartin, C., 2012. Subantarctic Mode and Antarctic Intermediate Water during the Present and Last Glacial Maximum. *Open Access Dissertations*. Paper 866.

IPCC, 2013. Summary for Policymakers. In: *Climate Change 2013: The Physical Science Basis. Contribution of Working Group I to the Fifth Assessment Report of the Intergovernmental Panel on Climate Change* [Stocker, T.F., D. Qin, G.-K. Plattner, M. Tignor, S.K. Allen, J. Boschung, A. Nauels, Y. Xia, V. Bex and P.M. Midgley (eds.)], 1–30.

IPCC, 2014. Climate Change 2014: Synthesis Report. *Contribution of Working Groups I, II, and III to the Fifth Assessment Report of the Intergovernmental Panel on Climate Change* [Core Writing Team, R.K. Pachuari and L.A. Meyer (eds.)]. IPCC, Geneva, Switzerland, 151 pp.

Ito, T., Woloszyn, M., Mazloff, M., 2010. Anthropogenic Carbon Dioxide Transport in the Southern Ocean Driven by Ekman Flow. *Nature*, **463**, 80-84, doi: 10.1038/nature08687.

Karstensen, J., and D. Quadfasel, 2002. Formation of Southern Hemisphere thermocline waters: Water mass conversion and subduction, *J. Phys. Oceanogr.*, **32**, 3020-3038.

Kirkman IV, C. H., and C. M. Bitz, 2011. The Effect of the Sea Ice Freshwater Flux on Southern Ocean Temperatures in CCSM3: Deep-Ocean Warming and Delayed Surface Warming. *J. Climate*, **24**, 2224-2237. doi: http://dx.doi.org/10.1175/2010JCLI3625.1

Long, M., K. Lindsay, S. Peacock, J. Moore, and S. Doney, 2013. Twentieth-Century Oceanic Carbon Uptake and Storage in CESM1(BGC). *J. Climate,* **26**, 6775–6800,
doi: 10.1175/JCLI-D-12-00184.1.

Marshall, J., D. Jamous, J. Nilsson, 1999. Reconciling thermodynamic and dynamic methods of computation of water-mass transformation rates, *Deep-Sea Research I*, *46*, 545-572.
doi: http://dx.doi.org/10.1016/S0967-0637(98)00082-X

Moore, J. K., K Lindsay, S. C. Doney, M. C. Long, and K. Misumi, 2013. Marine Ecosystem Dynamics and Biogeochemical Cycling in the Community Earth System Model [CESM1(BGC)]: Comparison of the 1990s with the 2090s under the RCP4.5 and RCP8 .5 Scenarios. *J. Climate*, **26**, 9291-9312, doi: http://dx.doi.org/10.1175/JCLI-D-12-00566.1.

Russell J. L., and A. G. Dickson, 2003. Variability in oxygen and nutrients in South Pacific Antarctic Intermediate Water. *Global Biogeochem Cy*., **17**, doi: 10.1029/2000GB001317.

Russell, J. L., Dixon, K. W., Gnanadesikan, A., Stouffer, R. J., and J. R. Toggweiler,
2006. The Southern Hemisphere westerlies in a warming world:
Propping open the door to the deep ocean, *J. Climate*, **19**(24), 6382-6390. doi: http://dx.doi.org/10.1175/JCLI3984.1

Sabine, C. L., R. A. Feely, N. Gruber, R. M. Key, K. Lee, J. L. Bullister, R. Wanninkhof, C. S. Wong, D. W. R. Wallace, B. Tilbrook, F. J. Millero, T. H. Peng, A. Kozyr, T. Ono, A. F. Rios, 2004: The oceanic sink for anthropogenic CO_2. *Science*, **305**, 367–371, doi:10.1126/science.1097403.

Shao, A. E., S.T. Gille, S. Mecking, and L. Thompson, 2015. Properties of the Subantarctic Front and Polar Front from the Skewness of Sea Level Anomaly. *J. Geophys. Res*., **120** , 5179-5193, doi: 10.1002/2015JC010723.

Sloyan, B. M., and I. V. Kamenkovich, 2007. Simulation of Subantarctic Mode and Antarctic Intermediate Waters in Climate Models. *J. Climate*, **20** , 5061-5080,
doi: http://dx.doi.org/10.1175/JCLI4295.1.

Sloyan, B. M., and Rintoul, S. R., 2001. Circulation, Renewal, and Modification of Antarctic Mode and Intermediate Water. *J. Phys. Oceanogr.,* **31**, 1005–1030,
doi: 10.1175/1520-0485(2001)031<1005:CRAMOA>2.0.CO;2.

Sloyan, B. M., L. D. Talley, T. K. Chereskin, R. Fine, and J. Holte, 2010. Antarctic Intermediate Water and Subantarctic Mode Water Formation in the Southeast Pacific: The Role of Turbulent Mixing. *J. Phys. Oceanogr.*, **40** , 1558-1574, doi: 10.1175/2010JPO4114.1.

Talley, L. D., 1999. Some aspects of ocean heat transport by the shallow, intermediate and deep overturning circulations. In Mechanisms of Global Climate Change at Millennial Time Scales, *Geophys. Mono. Ser.*, **112**, 1-22.

Talley, L. D., 2003. Shallow, intermediate and deep overturning components of the global heat budget. J. Phys. Oceanogr., **33**, 530-560.
doi: http://dx.doi.org/10.1175/1520-0485(2003)033<0530:SIADOC>2.0.CO;2

Weijer, W., B. M. Sloyan, M. E. Maltrud, N. Jeffery, M. W. Hecht, C. A. Hartin, E. van Sebille, I.Wainer, and L. Landrum, 2012. The Southern Ocean and Its Climate in CCSM4. *J . Climate*, **25**, 2652-2675, doi: http://dx.doi.org/10.1175/JCLI-D-11-00302.

Wunsch, C., D. Hu, and B. Grant, 1983. Mass, Heat, Salt, and Nutrient Fluxes in the South Pacific Ocean. *J. Phys. Oceanogr.*, **13**, 725-753,
doi: http://dx.doi.org/10.1175/1520-0485(1983)013<0725:MHSANF>2.0.CO;2.

Zhang, X., J. A. Church, S. M. Platten, D. Monselesan, 2014. Projection of subtropical gyre circulation and associated sea level changes in the Pacific based on CMIP3 climate models. *Clim Dyn*, **43**, 131-144, doi: 10.1007/s00382-013-1902-x